Wind Tunnel Testing on Negative-damped Responses of a 7MW Floating Offshore Wind Turbine

KARIKOMI Kai, KOYANAGI Takuya, OHTA Makoto, NAKAMURA Akihiro,
IWASAKI Satoshi, HAYASHI Yoshiyuki and HONDA Akihiro
Nagasaki Research & Development Center, Mitsubishi Heavy Industries, Ltd.
5-717-1, Fukahori-machi, Nagasaki, 851-0392, Japan
E-mail: kai_karikomi@mhi.co.jp Phone: +81-95-834-2385

Abstract

For pitch-controlled Floating Offshore Wind Turbines (FOWTs), the instability problem might occur by coupling of the floater pitch motion and the rotor speed control regulated by the blade pitch, which leads to adverse effect on the loads on the FOWTs. Some experiments related to scaled tank tests for FOWTs have been performed in recent years. To the best knowledge of the authors, however, there are few experimental studies where the unstable motion of FOWT due to the negative damping is clearly demonstrated by a tank or wind tunnel testing using a scaled FOWT model. On the other hand, there exist a number of papers which deal with the instability problem by using aeroelastic codes for FOWTs.

In this paper, we demonstrated experimentally the unstable motion of FOWT caused by the pitch control, and investigated effects of the gain parameters of the blade-pitch control on the behaviour of the floater pitch motion. Furthermore we validated an enhanced control method to suppress the negative damped response of the platform. The instability of the FOWT response in pitch motion depends on controller bandwidth. The negative damped response appeared in the cases with high controller bandwidth. Even for the controller bandwidth as high as the conventional fixed bottom turbines, we validated the enhanced control method to suppress the negative damped response of the platform.

1 INTRODUCTION

For pitch-controlled Floating Offshore Wind Turbines (FOWTs), the instability problem might occur by the coupling of the floater pitch motion and the rotor speed control regulated by the blade pitch [1]. This instability, which is well known as the negative damping, is caused by the fact that a thrust force loaded on the turbine rotor shows a negative slope against variations of wind speeds in rated power region. For a bottom-fixed wind turbine, the negative damping in the direction of fore-aft cannot appear because the tower natural frequency is an order of magnitude higher than the blade-pitch control bandwidth then the aerodynamic damping due to thrust shows positive most of the operation time. On the other hand, the negative damping can be problematic for a FOWT whose floater has a natural frequency almost equal to or lower than the blade-pitch control bandwidth and has very low hydrodynamic damping. The negative damping leads to large fluctuation of the floater pitch motion and then it has an adverse influence on integrity of the FOWT and fatigue loads on support structures. It is of great significance to assess the possibility of negative damping during the design process of FOWTs.

In this study, we performed wind tunnel testing on the negative damping responses and demonstrated experimentally the unstable motion of FOWT. In addition, the effect of the controller bandwidth on the behaviour of the floater pitch motion was investigated. Finally we validated an enhanced control method to suppress the negative damping.

2 WIND TUNNEL TESTING

2.1 Overview of wind tunnel testing

The objectives of this work are: 1) to realize the negative damping by wind tunnel testing, 2) to figure out effects of the control parameters on the stability of a FOWT, and 3) to validate an enhanced control

Table 1: Properties of wind tunnel test model

		Prototype	Wind tunnel model
Specification	Rated power	7,000 kW	3.3 W
	Rated rotational speed	10.3 rpm	82.4 rpm
	Rotor diameter	167 m	2.61 m
	Hub height	105.3 m	1.65 m
Controller		Variable-speed pitch regulated	
Floater		Advanced-spar-buoy type	
Fluid dynamic condition	Froude No.	equal	
	Reynolds No. (blade)	$5 - 9 \times 10^6$	$1 - 2 \times 10^4$

Figure 1: Wind tunnel test section

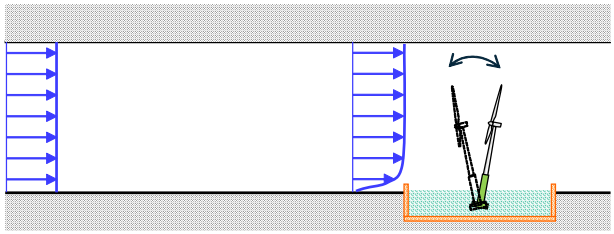

Figure 2: Schematic view of the wind tunnel and the water wank

method to suppress the negative damped response of the platform.

We conducted a series of wind tunnel tests at the Mitsubishi Heavy Industries, Ltd. wind tunnel facility, using a 1/64 scale 7MW FOWT model equipped with the blade pitch actuator to control the rotational speed of the rotor during the full load operation, as shown Tab.1. The floating platform used is categorized into the spar-buoy type. The wind tunnel is equipped with a small water tank, which enables wind and wave combined conditions.

2.2 Wind tunnel setup

Figure 1 shows the wind tunnel test section. The dimensions of the wind tunnel test section are the length of 30 m, width of 6 m and height of 5 m. This wind tunnel, utilized conventionally in the wind engineering field, can simulate the atmospheric turbulent boundary layer with the use of devices such as roughness blocks and spires. In order to perform scaled FOWT model testing, a water tank has been newly built on the floor of test section, as shown schematically in Fig.2. This square shaped water tank has dimensions of 4.5m width and 2.2 m depth. Regular waves can be generated by a wave-making device driven by a motor. It should be noted, however, that this paper presents only experimental results which were measured under conditions of no turbulence and no waves, due to limitations of space.

2.3 Aerodynamic problem due to Froude similitude

Scale model tests of FOWTs often raises the difficulty to properly scale hydrodynamic forces and aerodynamic forces simultaneously.

In this study on the negative damping, we focused on the pitch motion of FOWT as depicted in Fig.3. The simplified equation of motion for this case is described as Eq.1.

$$(I + A_{\text{radiation}})\ddot{\theta} + (C_{\text{radiation}} + C_{\text{viscous}})\dot{\theta} + K_{\text{hydro}}\theta = F_X H \tag{1}$$

Terms in the left hand side (LHS) are the mass inertia and added mass, the radiation damping and viscous damping, the restoring moment. The right hand side (RHS) is a aerodynamic moment caused by the rotor thrust. It is clear that the LHS is dominated by the Froude similitude whereas the RHS is

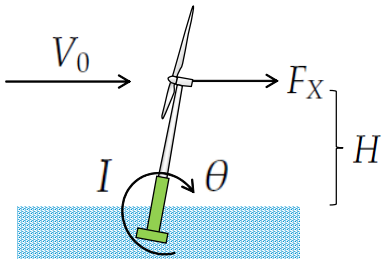

Figure 3: Illustration of 1 DOF pitch motion of FOWT

governed by the Reynolds similitude. Conventionally, model tests for FOWTs focuses on the motions of floating platform and the Froude similitude should be employed in order to properly scale the gravitational and hydrodynamic properties. However, as pointed out by [2], the Froude and Reynolds scaling cannot be satisfied simultaneously as described below, then the dominant equation of motion Eq.1 in scale testing with the use of a strictly-geometry scaled model might not be appropriately scaled relative to the real prototype scale.

When the Froude similarity rule is applied for this test, the Reynolds number is scaled to 1/512 compared to the real turbine, because the wind speed is proportional to square root of the dimension scale ratio according to the Froude similitude, and because the kinetic viscosity is constant for the real scale and model scale, then the Reynolds number should be proportional to $\sqrt{1/64} \times 1/64 = 1/512$. As a result, the Reynolds number of $5 - 9 \times 10^6$ in real scale decreases to $1 - 2 \times 10^4$ in test scale.

This very low Reynolds number causes serious aerodynamic problems; the Reynolds number with the order of 10^4, because of the laminar separation and the increased drag on aerofoils, results in definitely poor rotor performance and loads compared to the real turbine. In this study, to ensure the similarity of the test model's power and thrust with the real turbine, rotor blades were re-designed using thinner aerofoil and wider blades than the full scale prototype rotor.

2.4 Scale model

The scale model of wind turbine part is based on the MHI 7MW wind turbine whose properties are described in [6]. The floater part is modelled on the advanced-spar type floater designed by Japan Marine United [4]. The advanced spar is a axisymmetric floater composed of a column and hulls. Unfortunately, detailed information about this floater cannot be described here due to confidentiality. One of features of this floating structure is that although the shape is similar to a conventional spar-buoy typed floater, the draft is lower than the spar-buoy then easier to manufacture and install.

The dimensions of turbine and floater are on a scale of 1/64 to the prototype FOWT, except for the rotor blade dimensions such as the blade thickness, chord length and twist angle, as mentioned above.

For model testing of the floater motion of FOWT, it is of significance that masses of the model parts are manufactured so that they are proportional to the third power of the scale ratio. It is, however, not easy task because the scale model incorporates many sensing devices and cables connecting the sensors to data loggers, and their masses are comparable to the order of wind turbine parts. For example, a sensor with the weight of 100 g in wind tunnel becomes a 26 ton device in real scale. In this study, the tower top mass of model is 134% of the scaled mass of prototype FOWT, although many efforts were done such as the use of light-weight materials of carbon and aluminium, and the optimization of structure by using FEM. The difference of tower top mass can cause the difference of the natural period of floater motion. In order to practically equalize the FOWT model's the natural period of floater pitch motion to that of the prototype, the mass distribution of floater was tuned a little by adding small ballast.

Regarding vibration characteristics of the FOWT model, the structural properties of stiffness and damping of the rotor blades and tower were not scaled because this study only focuses on the unstable floater behaviour exerted by the turbine control.

2.4.1 Nacelle

Figure 5 shows the nacelle inside. The turbine model was designed to implement the variable-speed pitch regulated control in the same way as the prototype turbine. The nacelle incorporates a blade

Figure 4: FOWT model

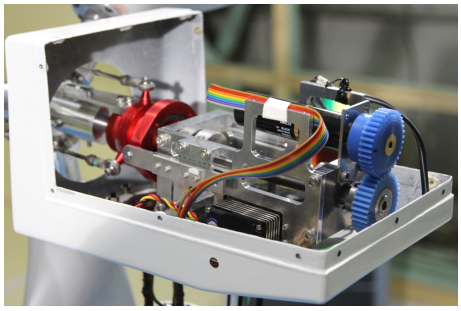

Figure 5: Nacelle inside

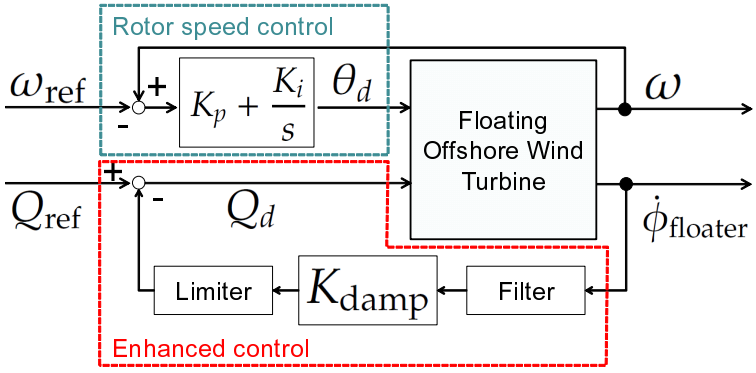

Figure 6: Schematic block diagram of enhanced control to suppress the negative damping

pitch actuator that can actuate the three blade pitch angles collectively according to control signals from a external controller unit. For use as a generator, an AC servo motor is implemented whose torque demand can also be variably set by the external controlling unit.

2.4.2 Baseline controller

The baseline control system has two conventional PI-regulators: the blade-pitch controller and the generator torque controller. In the full-load operation where the negative damping is expected to occur, this control system regulates the rotor speed and the generator torque to constant values. In this experiment, in order to investigate the influence of blade-pitch controller on the stability of floater motion, parametric study was performed varying the proportional gain K_p and integral gain K_i.

2.4.3 Enhanced control to suppress the negative damping

In order to avoid the negative damping, we have developed an enhanced controller as shown in Fig.6, inspired by the NMPZ(Non-Minimum Phase Zeros) compensation method [5]. Our design of the gain K_{damp}, filters and limiters are elaborately optimized to maximize the suppressing effect.

As derived by Fischer [5], the transfer function from the blade pitch angle to the rotor speed includes the aerodynamic term which is composed of the derivatives of thrust force and rotor torque with respect to the relative wind speed at the rotor. When this aerodynamic term has the negative sign and the absolute value of it is smaller than the hydrodynamic damping of the floater pitch, the floater pitch motion becomes unstable, resulting in the negative damping.

The enhanced controller suppress the unstable floater pitch motion by adding damping to the aerodynamic term in the transfer function. This damping term is provided by the feedback of the floater angular velocity to the generator torque demand. From the point of view of the control engineering, this additional damping corresponds to compensation of the non-minimum phase zeros of the transfer function expressing the rotor speed control loop.

2.5 Test cases

Test cases are divided into preliminary tests and main tests. In the preliminary tests, without the water tank, the scale model except the floater part is fixed on the wind tunnel floor likewise a onshore wind turbine, in order to figure out the steady performance of the re-designed rotor and the blade-pitch controller to regulate the rotor speed. Next, as the main tests, putting the scale model of FOWT including the floater on the water tank in the wind tunnel, the FOWT behaviour was measured to investigate effects of the various parameters of blade-pitch controller and to validate the enhanced controller.

Throughout all the test cases shown in this paper, the wind condition was set to quasi-uniform flow; the quasi-uniform flow here means the airflow generated over smooth surface without any roughness devices in the wind tunnel. Figure 7 shows longitudinal wind speed profiles of the wind tunnel speed of 1.5 m/s and 3 m/s, which covers wind speeds for the full load operation in the testing. The wind speeds are normalized by the wind speed at 1m height. There exists the wind speed deficit region below 0.5 m which can be regarded as the maximum height of the internal boundary layer generated on the floor. Above this height, the wind speeds are kept almost constant with the difference within 3%. Since there is the wind speed reduction in the region between the 0.5 m height and the lower rotor tip height of 0.34 m, it cannot be said that the inflow wind profile is strictly uniform. However, since the estimated area of the wind speed deficit part in the rotor plane is 0.6% compared with the entire rotor area of $5.35[\mathrm{m}^2]$, the wind speed profile can be regards as the quasi-uniform in terms of the performance measurement. The turbulence intensity is below 0.5%.

3 RESULTS AND DISCUSSIONS

3.1 Rotor performance

In order to evaluate the aerodynamic rotor power and thrust force of the re-designed rotor blades, the steady rotor performance was measured in the condition where the wind turbine part of the FOWT model, that is except for the floater, was fixed on the wind tunnel floor, as shown in Fig.8.

The reference wind speed was measured at a upstream position from the model to avoid the influence of rotor; the distance of the position is 5 times the rotor diameter.

The blockage of the rotor is not negligible because the rotor area and the test section area are $5.35[\mathrm{m}^2]$ and $30[\mathrm{m}^2]$ then the blockage ratio is 18%. The blockage effects on the performance and thrust coefficient were corrected according to Mikkelsen & Sørensen method [7].

The blade-pitch controller was not activated and the pitch angles were fixed during measurement runs. The rotor speed was also fixed to 82.4 rpm. Tip speed ratios were set to from 3 to 14 by changing the wind speed from 0.8 to 4 m/s.

The rotor performance and thrust coefficient are shown in Fig.9 and Fig.10. The power coefficient C_P varies with the change in pitch angles and reaches the maximum value of 0.32 at the tip speed ratio of 8.5 and the pitch angle of 0 deg. At this point, the thrust coefficient C_T is 0.88. This thrust coefficient value is almost same as the $C_T = 8/9 = 0.889$ obtained from the general momentum theory at a optimum rotor. Therefore the aerodynamic performance of the model rotor is found to be properly designed in spite of the low Reynolds number.

3.2 Steady power and thrust with the blade-pitch controller

Following the rotor performance testing, the steady operational power and thrust forces were obtained against various mean wind speeds. The model setup is the same as the previous rotor performance test except for the controller; the blade-pitch controller was activated for this case. The fine pitch angle was set to 0 deg. The reference rotation speed and rated torque were set to 82.4 rpm and 0.387 Nm, respectively.

Figure 11-13 show the measurement results of power, thrust force and pitch angle. These figures present scatter plots of time-averaged values. The rated wind speed at which the power reaches the rated power of 3.3 W is 1.5 m/s, which corresponds to 12 m/s in the real scale. Above the rated wind speed, the power is kept constant with the increase of pitch angles, which proves that the blade-pitch controller responds appropriately to the wind speed changes.

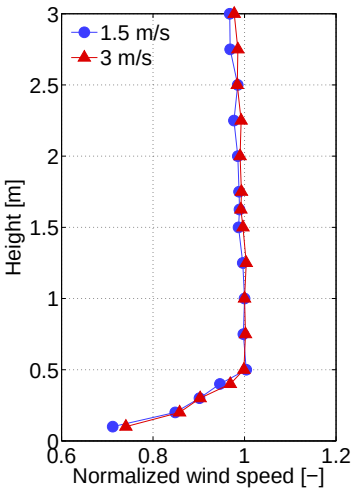

Figure 7: Vertical profile of longitudinal wind speed at the position of model

Figure 8: Setup for steady performance testing

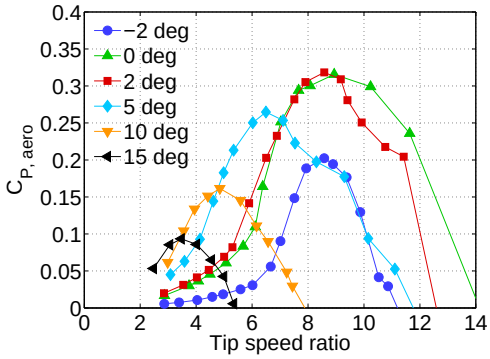

Figure 9: Aerodynamic power coefficient

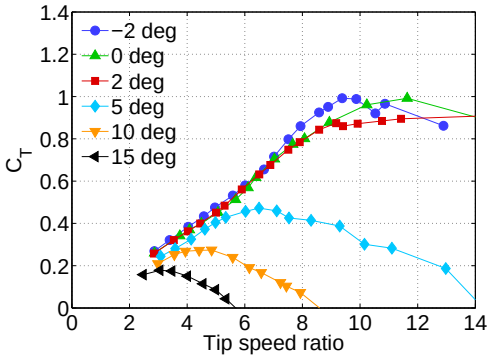

Figure 10: Thrust coefficient

In the full load operation region, the thrust force is decreased with the increase of wind speed; this negative slope of thrust is essential for occurrence of the negative damping of FOWT.

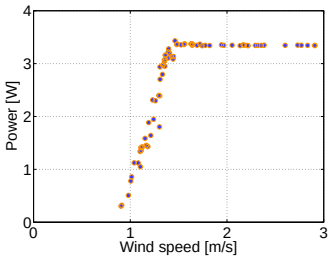

Figure 11: Power curve

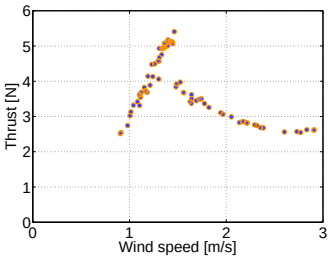

Figure 12: Thrust curve

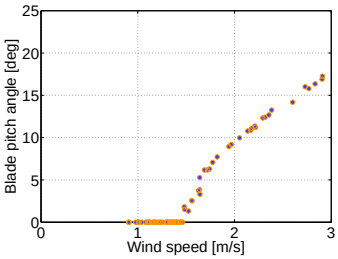

Figure 13: Pitch angle

3.3 Floating model tests

Next, putting the entire FOWT model including the floater on the water tank, the FOWT behaviour was investigated both for various gain parameters of the blade-pitch controller and for the enhanced controller to avoid the negative damping.

The set of gain parameters of the blade-pitch controller to be tested were determined by the following way. First, a baseline set of the proportional gain K_p and integral gain K_i of the controller were defined

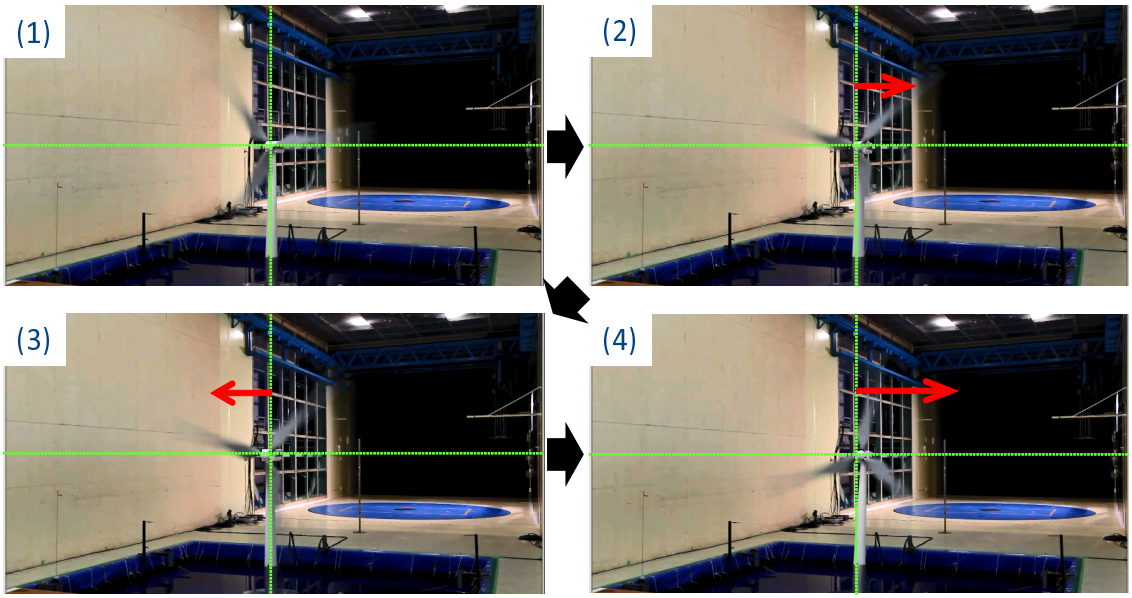

Figure 14: Snapshots of the negative damped floater pitch motion

by tuning these gains so that the response of the closed loop system were identical to that of the conventional bottom-fixed wind turbine in the real scale. Next, utilizing the model matching method, seven sets of the control gains were determined in order for their controller bandwidths f_{cb} to cover the range from the frequency of floater pitch motion f_{Floater} to higher frequencies than the frequency of floater pitch motion. The non-dimensional controller bandwidths of the seven sets, which are normalized by the f_{Floater}, range from 0.95 to 2.24.

The common test conditions for the floating model tests are the following: the wind speed of 1.8 m/s, in the still water (no wave), the fine pitch angle of 0°, the reference rotor speed of 82.4 rpm, the rated torque of 0.387 Nm, the rated power of 3.34 W.

3.3.1 Negative damping of FOWT

Without the enhanced controller, the negative damped responses were observed for five cases of the parametric study in terms of the controller gains for the blade-pitch controller. The highest controller bandwidth case showed significantly unstable motion of the FOWT; this case corresponds to the conventional settings for a bottom-fixed WT.

Figure14 shows the snapshots of the negative damped floater pitch motion for the highest controller case. The stop motions of the pitch oscillation presents that: (1)the floater pitch remained stationary with 2.5° at the measurement start; (2)(3)the FOWT began oscillation of pitch motion; (4)the amplitude of pitch motion was increasing with lapse of time and reached the limit cycle oscillation where the negative aerodynamic damping is considered to be balanced with the hydrodynamic damping of floater.

As shown in Fig.15 Case A, where the rotor speed controller gains are identical to the above case, the time series clarifies the signals of FOWT responses during the negative damping.

3.3.2 Controller bandwidth effect

In order to investigate the influence of the controller bandwidth on the stability of FOWT, the parametric study was performed changing the gains of blade-pitch controller. The FOWT responses observed in three representative cases are shown in Fig.15, where these three cases are set for the non-dimensional controller bandwidth of $f_{\mathrm{cb}}/f_{\mathrm{Floater}}$ equal to: 2.24 (Case A, high case), 1.68 (Case B, medium case) and 1.44 (Case C, low case). Here the controller bandwidth f_{cb} is normalized by the natural frequency of the floater pitch motion f_{Floater}. The time axis is also non-dimensionalized by measurement periods. It should be noted that Case A can be regarded as the conventional setting for the bottom-fixed wind turbine; this Case A is identical to that shown in Section 3.3.1.

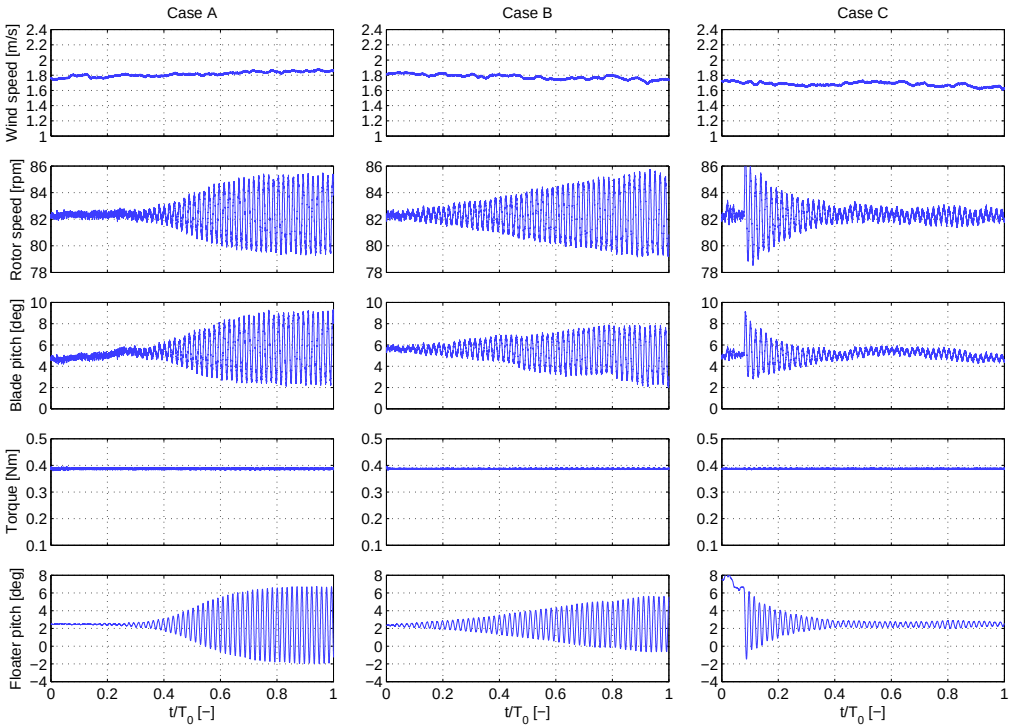

Figure 15: FOWT responses for the selected three cases of controller bandwidth $f_{\mathrm{cb}}/f_{\mathrm{Floater}} = 2.24$ (left: Case A), 1.68 (center: Case B), 1.44 (right: Case C)

The stability of FOWT is apparently affected by the controller bandwidth. For the highest bandwidth Case A, the amplitude of floater pitch motion rapidly increased and converged to the limit cycle, whereas for the middle bandwidth Case B the amplitude growth rate of the pitch motion is slower then Case A. Only for the lowest bandwidth Case C, at the start of measurement, the initial floater pitch angle of 6° was given by pulling a string connected to the tower top, and subsequently releasing it in order to obtain the decay response of floater. This is because, with this controller bandwidth, the response of pitch regulation against fluctuations of the relative inflow speed to the rotor is slow enough to give positive aerodynamic damping to the FOWT.

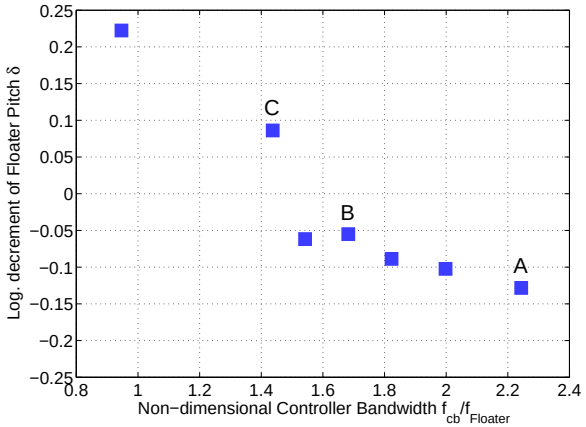

Figure 16: Effect of the blade-pitch controller bandwidth on the stability of floater pitch response

To quantitatively figure out the controller bandwidth effect on the floater motion, as index of the stability, the values of logarithmic decrement were estimated from envelopes fitted to the time series of floater pitch fluctuations for each measurement case. The logarithmic decrement δ with negative sign

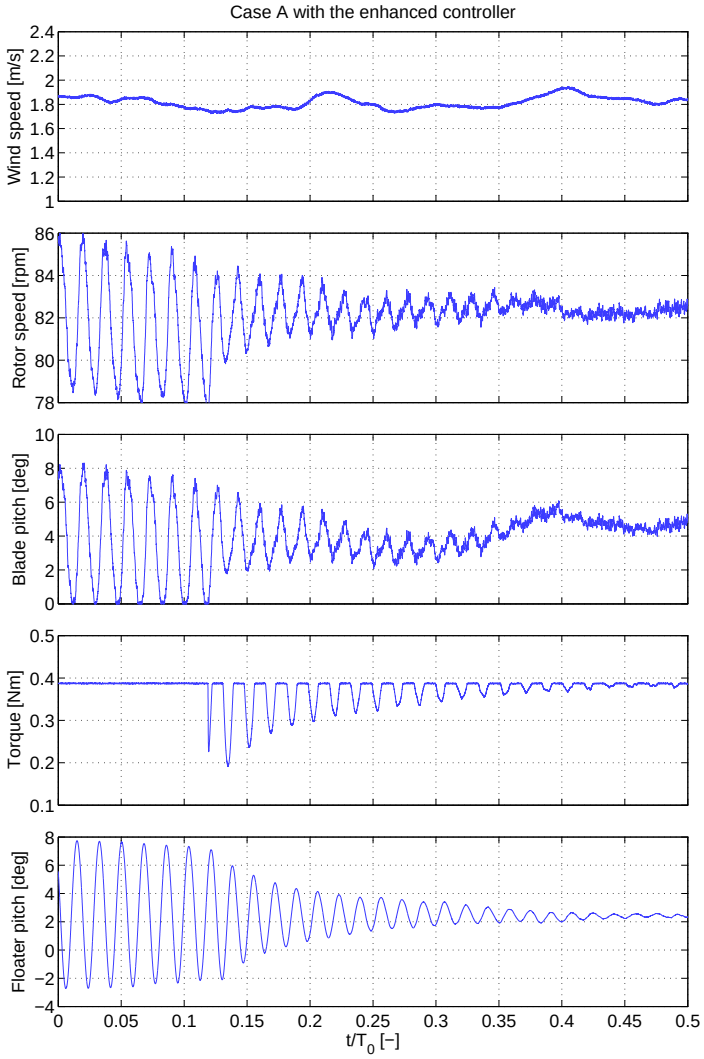

Figure 17: Effect of the enhanced controller on the FOWT response; with the enhanced controller added to the conventional blade-pitch controller gains Case A

represents the negative damping like Case A and B; the positive δ means that the FOWT is positively damped and stable like Case C.

Figure 16 clearly explains the influence of the controller bandwidth, where the logarithmic decrements are plotted against the normalized controller bandwidth. The aforementioned three cases A, B and C are marked with the case names in this plot.

The higher bandwidth than around 1.5 causes the unstable motion of the FOWT, whereas the lower bandwidth stabilizes the floater motion. Although decreasing the blade-pitch controller bandwidth to the natural period of floater has positive effect on the stability, it could increase the rotor speed fluctuation as a trade-off [5]. Hence reduction of the blade-pitch control gains could not be practical in terms of actual control for a real turbine.

3.3.3 Validation of the enhanced controller

The enhanced controller that we have developed can suppress the negative damped response of the floater, instead of decreasing the gains of blade-pitch controller.

The observed response of FOWT is shown in Fig.17 where the enhanced controller was applied together with the blade-pitch controller gains of Case A. In this case, the measurement started only with the blade-pitch controller gain Case A and without the enhanced controller. That is why, during the

initial stage of the measurement, the floater pitch motion shows the limit cycle oscillation resulted from the negative damping. It is clear that after the enhanced controller was switched on at $t/T_0 = 0.12$, the floater pitch motion was rapidly stabilized.

The enhanced controller absorbs the fluctuation of the energy flux of inflow into the rotor by use of the torque control which provides feedback of the floater angular velocity to the generator torque demand; that fluctuation of the energy flux of inflow is exerted by the conventional pitch-regulated rotor speed control. According to the above mechanism, immediately after the activation of enhanced controller, the torque began to fluctuate and the floater pitch motion became positively damped together with the rotor speed and blade pitch. Finally, after $t/T_0 = 0.45$, the fluctuating torque and floater pitch almost converged with the steady state.

The logarithmic decrement estimated for this case is $\delta = 0.18$ with the non-dimensionalized blade-pitch control bandwidth of 2.24 being the same as Case A. This fact confirms that FOWTs can operate without the occurrence of negative damping in spite of the similar bandwidth of the blade-pitch controller to the fixed-bottom wind turbine, if the enhanced controller to suppress the negative damping is applied. It should be also noted that, in actual situations for the real turbine, if this enhanced controller was activated all the time, there would be no occurrence of such large fluctuations of the torque, the rotor speed and the floater pitch motion that were observed in the experimental demonstration case as shown above.

4 CONCLUSIONS

We investigated effects of the gain parameters of the blade-pitch controller on the behaviour of the floater pitch motion. It was demonstrated that the instability of the FOWT response in pitch motion was dependent on controller bandwidth and the negative damped response appeared in the test cases with high controller bandwidth.

Even for the controller bandwidth as high as the conventional fixed bottom turbines, we validated the enhanced control method to suppress the negative damped response of the floating platform.

References

[1] Larsen, T.J. and Hanson, T.D., "A method to avoid negative damped low frequent tower vibrations for a floating, pitch controlled wind turbine," Journal of Physics: Conference Series 75 (2007) 012073, 2007.

[2] Martin, H.R., "Development of a Scale Model Wind Turbine for Testing of Offshore Floating Wind Turbine Systems," Electronic Theses and Dissertations. Paper1578, The University of Maine, 2011.

[3] William E-J.R et al., "State of the Art Model Testing Techniques for Floating Wind Turbines," EWEA Offshore 2013.

[4] Yoshimoto, H. et al., "Development of floating offshore substation and wind turbine for Fukushima FORWARD," Proc. International Symposium on Marine and Offshore Renewable Energy, 2013, Tokyo, Japan.

[5] Fischer, B., "Reducing rotor speed variations of floating wind turbines by compensation of non-minimum phase zeros," EWEA 2012.

[6] Karikomi,K. et al., "Hydrodynamic analysis of a 7MW floating offshore wind turbine," EWEA Offshore 2013.

[7] Mikkelsen,R., "Actuator disc methods applied to wind turbines," MEK-FM-PHD 2003-02, Fluid Mechanics, Department of Mechanical Engineering, Technical University of Denmark, 2003.